Impact of pressure on the dynamic behavior co2 hydrate slurry during storage process

T. Dufour, J. Oignet, Hong-Minh Hoang, Denis Leducq, Anthony Delahaye,
Laurence Fournaison, M. Pons

IMPACT OF PRESSURE ON THE DYNAMIC
BEHAVIOR OF CO$_2$ HYDRATE SLURRY DURING STORAGE
PROCESS

Thomas Dufour [(a)], Jérémy Oignet [(a)], Hong Minh Hoang [(a)], Denis Leducq [(a)], Anthony Delahaye [(a)],

Laurence Fournaison [(a)], Michel Pons [(b)]

[(a)] Irstea, UR GPAN, 1 rue Pierre-Gilles de Gennes, 92761 Antony, France

[(b)] LIMSI, CNRS, Université Paris-Saclay

ABSTRACT

Two-phase fluids are considered as high-performance fluids for secondary refrigeration thanks to high energy density of phase change material (PCM). Nevertheless, one limitation in such system is thermal energy storage dynamic, in particular PCM charging/discharging rate, which depends generally on fluid temperature and flow rate. In the present work, the influence of pressure on the charging/discharging processes of gas hydrates has been studied experimentally using a stirred tank reactor. A model of stirred tank reactor was also developed and validated. The results showed that pressure can be used to adjust gas-hydrate phase-change temperature and consequently to improve charging/discharging time. For the same working conditions (temperature, flow rate, charging time…), the amount of stored energy using gas hydrates at 3 MPa is two times higher than that using water. The model was used to compare gas hydrates slurries to other slurries at ambient pressure.

Keywords: hydrate slurry, CO$_2$, heat transfer, modelling, thermal energy storage

1. Introduction

Nowadays, cold production has an important impact on the environment. 80 % of the pollution caused by cold production is due to the energy consumption of the installations and 20 % are caused by the leakage of the refrigerant gas (mainly HFC), which are greenhouse-effect gases. Secondary refrigeration is known as a solution to reduce the use of primary refrigerant fluids (Fournaison *et al.* 2000) : cold production is still carried out by classical refrigerant fluid in a smaller loop but cold storage and transport is now carried out by an environment-friendly secondary fluid (in a second loop. In order to increase the storage capacity of the secondary fluid, phase change material (PCM) slurries can be used such as ice, paraffin, or hydrate slurries (Koh *et al.* 2012) (Zhang *et al.* 2012) . Hydrates are solid particles able to trap guest molecules such as gas or salt (Sloan 1998; Sloan *et al.* 2008). They are formed at positives temperatures and under pressure in the case of gas hydrates (Mao *et al.* 2007). Their high energy density (374 kJ.kg$^{-1}_{hyd}$ for CO$_2$ hydrates) (Marinhas *et al.* 2006), higher than that of ice (333 kJ.kg^{-1}), makes them very attractive for cold storage (Fournaison *et al.* 2004). In addition, the relatively low viscosity of hydrate slurries is interesting for cold transportation (Delahaye *et al.* 2011; Youssef *et al.* 2013) in the field of refrigeration (Delahaye *et al.* 2008) (Jerbi et al., 2013)

The present article is focused on the importance of pressure on hydrate slurry formation using experimental and modelling investigation in a stirred tank reactor. The storage dynamic of system using water and CO$_2$ hydrates was analyzed to evaluate the interest of phase change. In fact, the use of PCM as hydrates instead of liquid water is generally justified by the increase of the storage capacity. Nevertheless, this improvement is not necessarily interesting if it leads to an increase of the charging time. In the case of CO$_2$ hydrate, pressure can be used to adjust theoretically phase change temperature, and potentially to improve storage dynamic. The objective of this study is to assess the impact of pressure on operating conditions (thermodynamics, kinetics) in a stirred tank reactor used to form hydrate slurries. Based on experimental data, a tank model was

developed and validated in order to describe storage parameters (capacity, charging time) and finally to estimate the relationship between pressure (and temperature) conditions and storage dynamic. The model development is based on finite volume method: heat flux balance was applied on each node of the mesh; an implicit scheme is used for time discretization. The model, validated for CO_2 hydrates, can be applied for other types of hydrates. In this work, a comparison between TBPB and CO_2 hydrates has been also presented. Thanks to this model the impact of latent storage can be observed in terms of energy efficiency. A comparison between water storage and hydrates storage will be made in term of energy but also in term of heat exchange. The first results have shown a good agreement between experimental. Moreover the energy study shows that in addition to increasing stored energy the presence of hydrates improve storage dynamics by doubling the amount of stored energy during the same time.

2. Material and methods

In order to study CO_2-hydrate-slurry formation dynamic, a pilot loop (Figure 1a) previously developed (Jerbi *et al.* 2010; Jerbi *et al.* 2013) has been used. This loop can be divided into three parts: a tank reactor to form hydrate slurry, a circulation loop in which the slurry's rheological and heat transfer behaviors can be analyzed, and a heat exchanger to study CO_2 hydrate dissociation. This paper is focused on hydrate slurry formation in the tank reactor (Figure 1b).
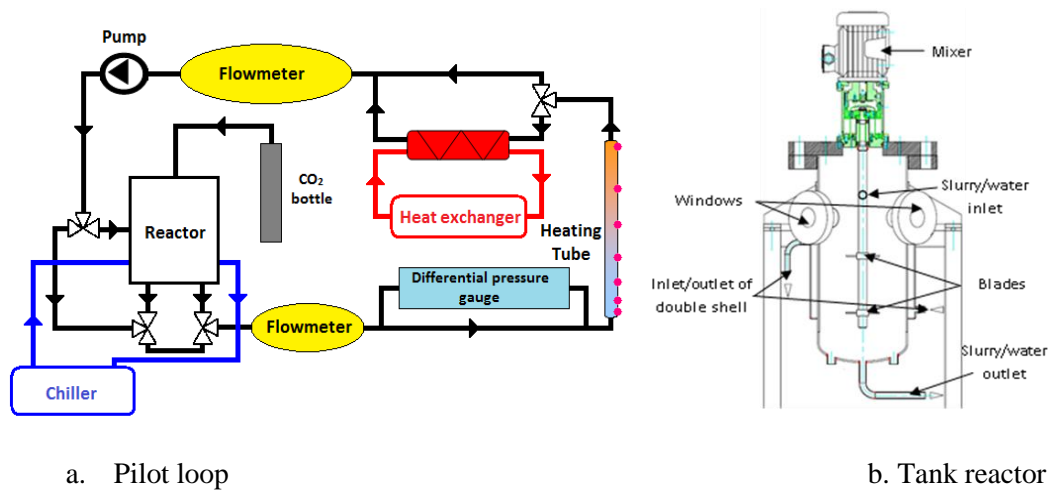

| a. Pilot loop | b. Tank reactor |

Figure 1: Pilot loop and tank schemes

2.1. Formation tank

The formation tank (Figure 1b) is a stainless steel reactor with a capacity of 26.47 L equipped with two glass windows in order to observe hydrate formation. The reactor is able to support a pressure up to 4.5 MPa. The tank is thermostated using a cooling jacket connected to a chiller (263.15-293.5K). Two thermocouples were installed to measure the inlet and outlet temperatures of the cooling fluid so that the heat removed from the tank can be quantified. A magnetic entrainment mixer (Burgmann MAK, power: 0.55 kW) is fixed at the top of the tank and used to improve heat transfer between the reactor and the cooling jacket; to enhance CO_2 absorption in liquid phase; to homogenize the slurry; and to prevent hydrate crust formation at the gas-liquid interface. The reactor is connected to a CO_2 bottle by two inlets, one on the top and one on the bottom of the tank so that CO_2 can be injected in the vapor phase or in the liquid to improve CO_2 absorption. The reactor is connected to the circulation loop by one outlet located on the bottom of the reactor and one inlet on the top. The reactor is instrumented with: three PT 100 (± 0.3K) at the top to measure vapor phase temperature, at the bottom and at the middle of the reactor to measure liquid phase temperature, two pressure probes (0–5 MPa, $\pm 0.05\%$ of full scale) at the top and the bottom.

2.2. Hydrates formation on the experimental set up

Initially, the reactor contains water-CO_2 mixture in liquid-vapor state at 282 K and in a range of pressure between 1 to 3.4 MPa. After reaching the equilibrium dissolution of CO_2 in water, the reactor is cooled. Hydrate formation is performed in a closed system so that the total amount of CO_2 can be determined with initial data.
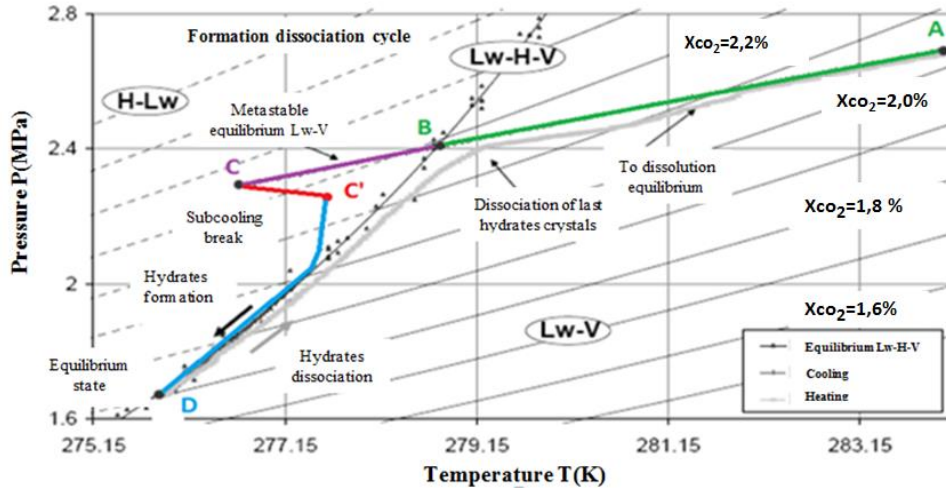

Figure 2: CO_2-water phase diagram

During the first stage of cooling, the aqueous solution is in the L_w-V field of the (P,T) diagram (A -B, Figure 2). When the system reaches the liquid-hydrate-vapor (L_w-H-V) equilibrium curve, hydrates are not formed immediately because of a sub cooling degree reflecting the metastable liquid-vapor equilibrium, the system continues to be cooled but in the Hydrates-Liquide (H-L_w) region (B-C).The time during which the system stays in a metastable state in the H-L_w phase is called induction time and corresponds to the needed time to form a first stable hydrate crystal. At point C, a rupture of metastability occurs and causes a sudden increase of system temperature and a pressure drop (point C'). These phenomena result from the exothermic and CO_2-consuming hydrate-formation. After this rupture, the system reaches the L_w-H-V curve and follows it for the remaining time of cooling (C-D Figure 2). The final condition is reached when system's temperature is in steady state; this temperature is chosen to be greater than 273.15 K, in order to avoid ice formation.

2.3. Reactor modelling

The tank reactor has been modelled in order to study the storage dynamic. The heat exchange between the reactor, the cold source and the environment has been modelled using the finite volume method. The reactor was divided in sixteen parts: six for fluid phase to simulate different height of filling, six corresponding parts for wall temperature and four for the cover. The wall has not been divided in the widthwise because of its low thickness and its high conductivity.
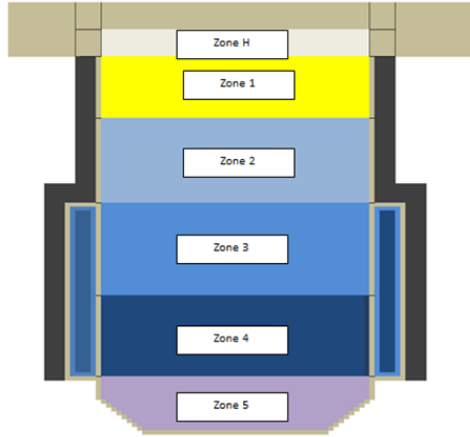
Figure 3 gives a representation of the tank segmentation.

The energy balance is applied on each node (fluid and wall parts) of the tank: the change of heat accumulated for each node (index j) (ϕ_{accu}) is determined by the sum of heat conduction and convection flux (ϕ_{cond} and ϕ_{conv}) with the surrounding nodes (index s):

$$\dot{Q}_{stored} = \sum \phi_{cond} + \sum \phi_{conv} \qquad (1)$$

with $\dot{Q}_{stored} = m_j C_{p-ap} \dfrac{dT_j}{dt}$; $\;\Sigma \phi_{cond} = \sum\limits_s \dfrac{T_j^{i+1} - T_s^{i+1}}{R_{cond,js}}$; $\;\sum \phi_{conv} = \sum\limits_s \dfrac{T_j^{i+1} - T_s^{i+1}}{R_{conv,js}}$; i is the time index;

$R_{cond,js}$ and $R_{conv,js}$ are thermal resistances. Hydrate phase change is considered using the apparent heat capacity:

$$C_{p-ap}(T) = \frac{\Delta H d\varphi + Cp_L(1-\varphi)dT + Cp_s \varphi dT}{dT} \qquad (2)$$

Figure 3: Representation of the tank and its different parts

2.4. Evaluation of CO₂ hydrates formation

In order to quantify the amount of formed hydrate at each time, the correlation of (Marinhas et al. 2006) based on a CO_2 mass balance in its various phase at equilibrium (vapour, dissolved in liquid and enclathrated) was used:

$$n_h = \frac{n_{CO_2,tot} - \sigma_{CO_2} \dfrac{\rho_{H_2O} V_l}{M_{H_2O}} - (\dfrac{P_{CO_2}}{Z(P_{CO_2},T)TR})(V_{tot} - (n_{H_2O,l} - nb_h n_h)(M_{H_2O} + \sigma_{CO_2} M_{CO_2}))}{1 - \sigma_{CO_2} nb_h + (\dfrac{P_{CO_2}}{Z(P_{CO_2},T)TR})((nb_h n_h)(M_{H_2O} + \sigma_{CO_2} M_{CO_2}) - \dfrac{M_h}{\rho_h})} \qquad (3)$$

2.5. Evaluation of TBPB hydrates formation

In this work, TBPB hydrates (at atmospheric pressure, without CO_2) are considered for comparison with CO_2 hydrates (depending on pressure). The evaluation of TBPB hydrate amount and the residual liquid-phase composition is based on the momentum law (TBPB mass balance). These data depends on the initial TBPB concentration and phase change temperature, which varies in function of the TBPB concentration in the liquid phase according to the following equation:

$$Tcc = A(1 - e^{-k*(x-xc)}) - 273.15 \qquad (4)$$

Where A and k are coefficients which depend on TBPB concentration and on CO_2 differential pressure..

2.6. Evaluation of stored energy

The stored energy in hydrate slurry depends on hydrate phase change, hydrate cooling, and liquid cooling. It can be determined by the integration of the change in heat accumulated in the fluid (equation 1 and 2) during the cooling process:

$$Q_{stored} = \int_0^t \dot{Q}_{stored} dt \qquad\qquad (5)$$

With a view to comparing the storage efficiency between hydrates (various mass fractions) and water, the stored energy and the charging time are normalized by the maximum of stored energy with water Q_{w-max} and the time required for water to attain this quantity t_{w-max} as shown in equations (5) and (7).

$$Q_{norm} = \frac{\int_0^t \dot{Q}_{stored} dt}{Q_{w-max}} * 100 \qquad\qquad (6)$$

$$t_{norm} = \frac{t}{t_{w-max}} \qquad\qquad (7)$$

The improvement of stored energy should not be accompanied with an increase of the charging time. Thus, an average charging rate is defined and can be considered as a criterion of efficiency:

$$\dot{Q}_{av} = \frac{\int_0^t Q_{stored}}{t} \qquad\qquad (8)$$

3. RESULTS AND DISCUSS

At first, the model was validated with experimental data in reactor obtained for CO_2 hydrate formation. Then, the results on storage dynamics for three kinds of storage (water, CO_2 and TBPB hydrates) are presented and discussed.

3.1.   Model validation

As previously described, the modeling of hydrate slurry takes into account heat transfer, phase change and pressure evolution. The model was applied on the stirred tank reactor for three different initial pressures (25, 27 and 29 bar) leading to the formation of different hydrates fractions.
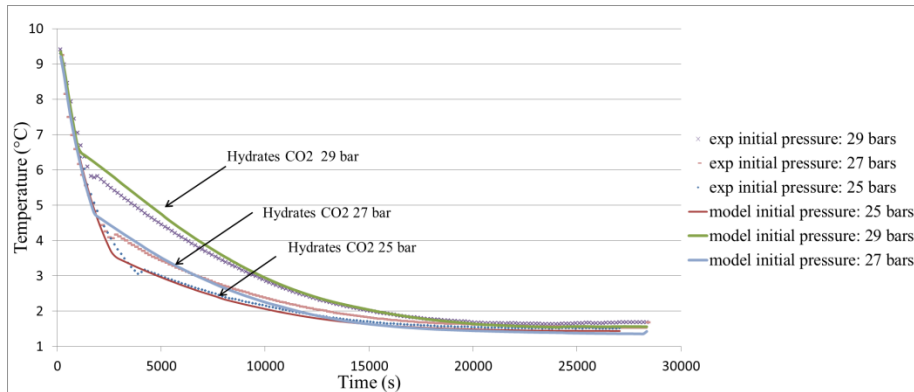
Figure 4: Comparison between experimental and numerical temperature for CO_2 hydrates

The experimental and modelled temperature evolutions of the solution inside the reactor are represented on Figure 5. Fluid temperature is supposed to be homogeneous thanks to the mixer. Temperature evolution can be divided into three stages: cooling (before hydrate formation), hydrate formation, and stationary state. The cooling stages are the same for all cases. However, hydrates formation condition is reached at higher temperature with a higher initial pressure which can be explained by the phase diagram (Figure 2). A larger gap between the experimental and numerical data can be observed during hydrate formation stage because the subcooling is neglected in the modelling. At the stationary state, slurry temperature is nearly the same for all cases, the final mass fractions are 10%, 18% and 21% for the three corresponding initial pressures (25, 27

and 29 bar). It can be observed that the model predicts well the experimental data with an average error of 0.2K.

3.2. Evaluation of storage dynamic

3.2.1. CO_2 and TBPB hydrates

In order to compare CO_2-hydrate slurry formation with another type of slurry, the model was used to simulate TBPB hydrate formation. TBPB hydrates have been chosen due to their equilibrium temperatures equivalent to those of CO_2 hydrates. The comparison in temperature evolution is presented on
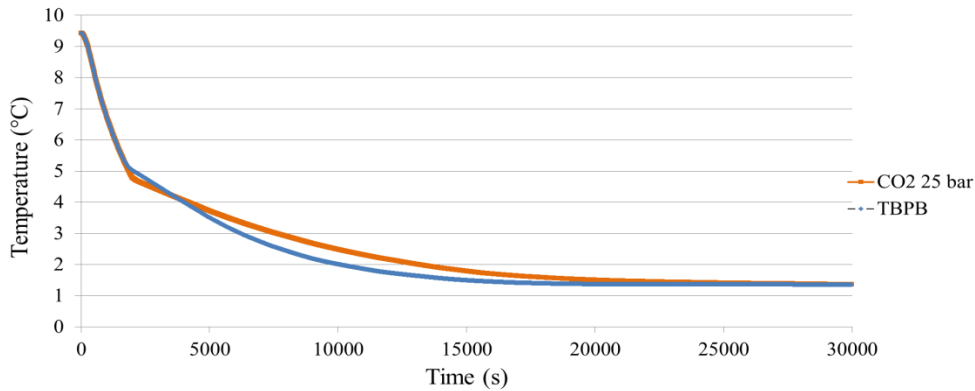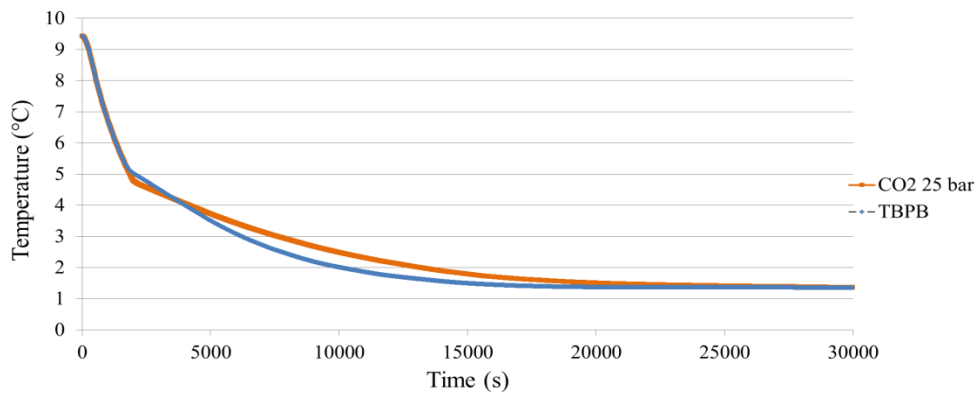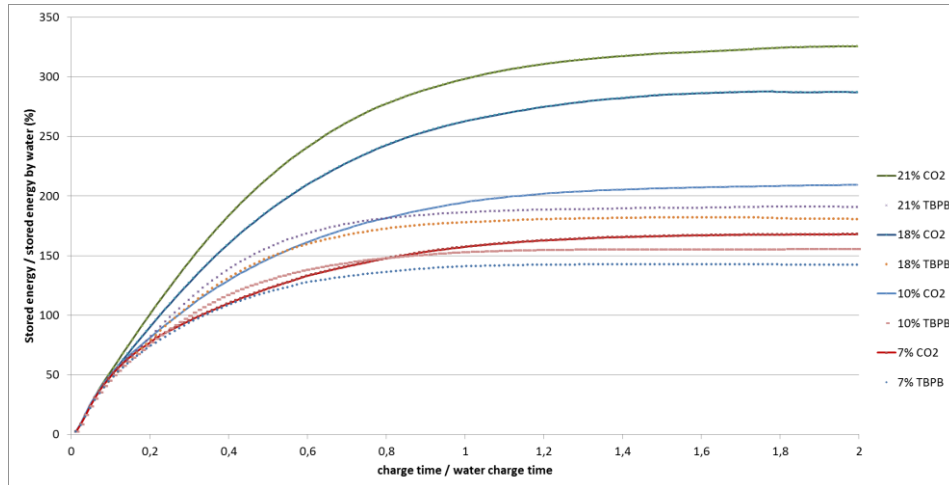

Figure 5.

Figure 5: Comparison of the temperature evolution of TBPB and CO_2 hydrates slurries during formation (numerical results)

It can be observed that the solution with TBPB hydrates reaches its final temperature faster than CO_2 hydrates. This difference on system dynamics is due to the lower latent heat of TBPB hydrates that facilitates the cooling of the reactor. Nevertheless, the aim of this cooling is not to reach a final temperature but to store a maximum of energy in a minimum time. In order to compare the two slurries, an energy analysis has to be realized. By convention, systems with different initial conditions are compared in function of the final fraction (which is reached when the system attains its stationary state) other than using parameters such as initial pressure or initial salt fraction.

3.2.2. Influence of the mass fraction on stored energy

The figure 6 presents the evolution of the stored energy in function of the charging time for 4 CO_2 and TBPB hydrates mass fractions: 7, 10, 18 and 21%.

Figure 6: Normalized stored energy for CO_2 and TBPB hydrate slurry (numerical results)

In order to facilitate the comparison between latent and sensible storages, the energy stored in hydrates and the charging time have been normalized by the final energy stored in water and the corresponding charging time (equations (5) and (7)). For the same charging time (t_{norm}=1), the energy stored in CO_2 (or TBPB) hydrate slurry with hydrate mass fraction of 18% is 2 (1.7) times greater than that of liquid water. For both hydrates and for all of the final fractions, the stored energy is greater than with water.

This higher value is due to phase change which stabilizes solution temperature. This thermal stabilization allows a better heat exchange between cold source and the reactor and improves storage rate. This phenomenon is improved with the increase of pressure, and thus the increase of phase change temperature and hydrate fraction. It is also noticeable that the full charge time (t_{norm}= 2) is equivalent for all the system.

Moreover the energy stored during the same charging time with CO_2 hydrates is greater than with TBPB hydrate due to a higher phase change enthalpy which can be observed in Table 1.

Table 1: Stored energy of water, TBPB and CO_2 hydrates (numerical results)

Time\Energy (kJ)	Water	7% CH	7% TBPB	10% CH	10% TBPB	18% CH	18% TBPB	21 % CH	21% TBPB
0.5	345	374	358	393	369	435	379	486	393
1	442	530	523	620	566	763	630	875	664
2	483	716	666	881	724	1 172	842	1 344	887

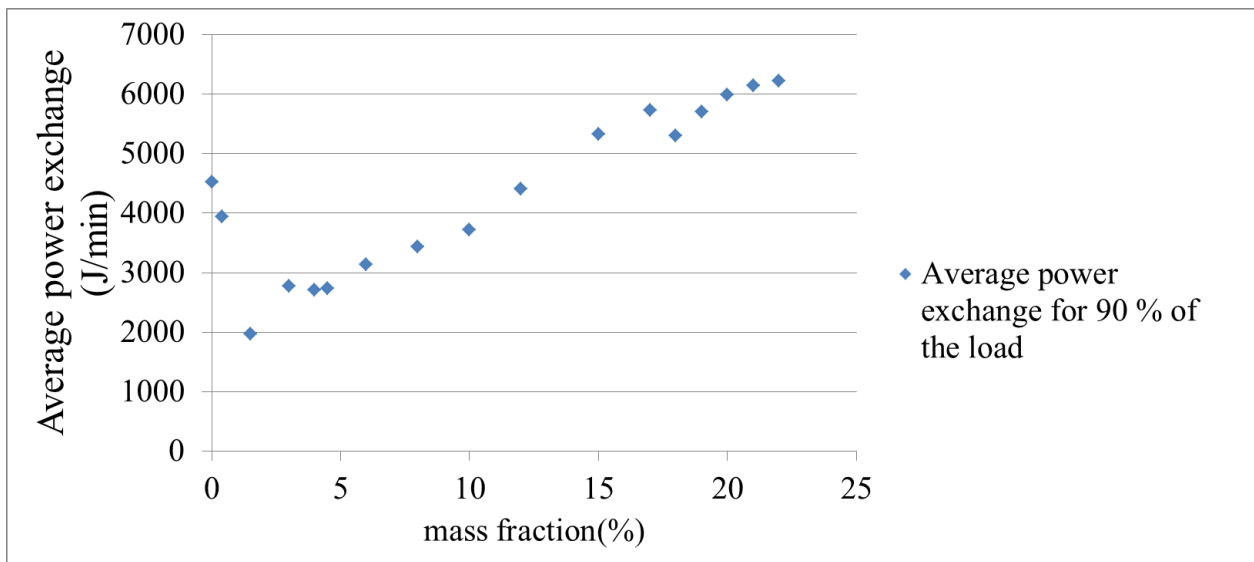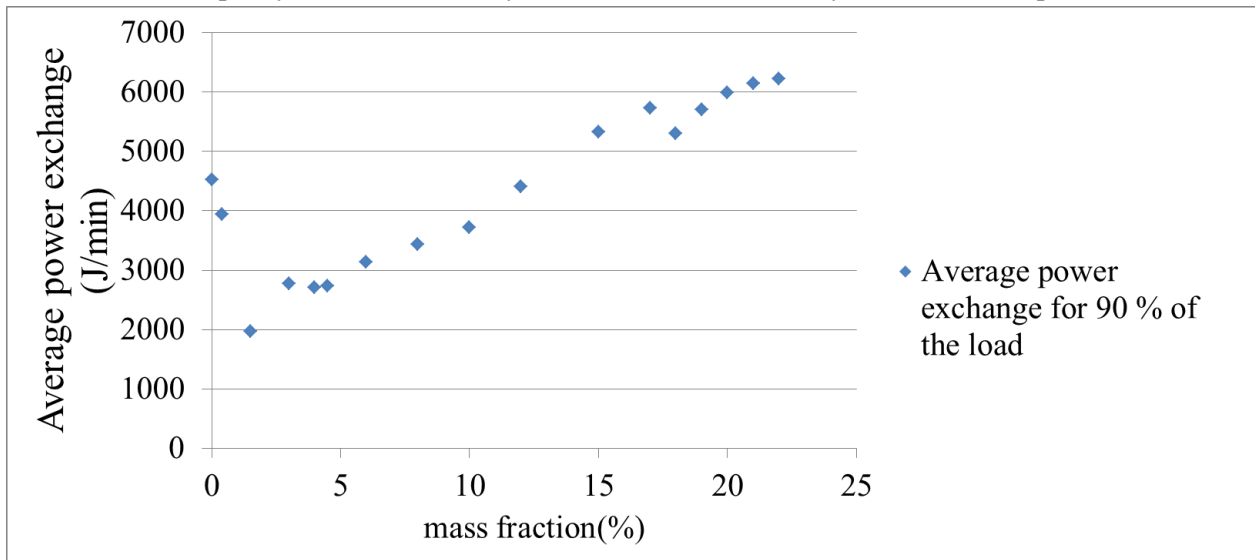**3.2.1.** Influence of hydrate mass fraction on average charging rate

Figure 7 shows the experimental data for average charging rate (defined by equation 9) for a storage capacity 90% of maximal capacity for various CO_2 hydrates fractions obtained by different initial pressures.

Figure 7: Average charging rate in function of hydrates fractions (experimental data)

The results show that for low hydrate fraction (<10%), the charging rate is lower than that of water (4500 J.min^{-1}) because of a low phase change temperature so that most of the storage is realized with a little temperature difference between the solution and the cooling fluid. However for medium and high fractions (from 15 to 20%) which correspond to higher initial pressure, not only the amount of stored energy is increased but also the charging rate and thus system efficiency.

4. Conclusion

The impact of pressure on hydrate slurry formation in a stirred tank reactor has been studied by using experimental investigations and modelling development. The model was validated thanks to experimental data and was used to compare in various conditions a liquid water system and 2 types of hydrate slurries using CO_2 (under pressure) or TBPB (atmospheric pressure). According to numerical results, both CO_2 and TBPB hydrates at various fractions have a greater stored energy than water, which is an expected result from system using a phase change process. Moreover, the energy stored during the same charging time (corresponding to a thermal power) with CO_2 hydrates is greater than with TBPB hydrate, in particular due to a higher phase change enthalpy. Concerning CO_2 hydrates, the results showed that the increase of the initial pressure allows: an increase of hydrate fraction and the amount of stored energy, but also an increase of

phase change temperature and thus a better heat exchange with the cold source. The analysis in term of average charging rate for a 90% full storage shows that the storage efficiency can be improved by hydrates at relatively high fraction (greater than 15%). As a nutshell, the use of CO_2 hydrate slurry can be a good solution to improve not only the amount of energy stored but also the charging time and thus the thermal power exchanged between hydrate slurry and a cold source.

NOMENCLATURE

m	weight, *kg*	Q	energy, *J*		*Subscripts*
Cp	specific heat, *J.kg^{-1}.K^{-1}*	ΔH	Phase change entalpie, *J.kg^{-1}*	l	liquid
T	temperature, *K*		*Greeks symbols*	h	hydrate
x	TBPB mass fraction	φ	Hydrates mass fraction	w	Water
nbh	Hydratation number	ϕ	flux, *W*	c	stoechiometric
t	times, *s*	σ	Solubility		

5. References

Delahaye, A., Fournaison, L., Jerbi, S.,Mayoufi, N. 2011. Rheological Properties of CO2 Hydrate Slurry Flow in the Presence of Additives. Industrial & Engineering Chemistry Research **50**(13): 8344-8353.

Delahaye, A., Fournaison, L., Marinhas, S.,Martinez, M. C. 2008. Rheological study of CO2 hydrate slurry in a dynamic loop applied to secondary refrigeration. Chemical Engineering Science **63**(13): 3551-3559.

Fournaison, L., Delahaye, A., Chatti, I.,Petitet, J. P. 2004. CO$_2$ hydrates in refrigeration processes. Industrial & Engineering Chemistry Research **43**(20): 6521-6526.

Fournaison, L.,Guilpart, J. 2000. Frigoporteurs monophasiques ou diphasiques ? Revue générale du froid **1001**: 21-24.

Jerbi, S., Delahaye, A., Fournaison, L.,Haberschill, P. 2010. Characterization of CO2 hydrate formation and dissociation kinetics in a flow loop. International Journal of Refrigeration **33**(8): 1625-1631.

Jerbi, S., Delahaye, A., Oignet, J., Fournaison, L.,Haberschill, P. 2013. Rheological properties of CO2 hydrate slurry produced in a stirred tank reactor and a secondary refrigeration loop. International Journal of Refrigeration **36**(4): 1294–1301.

Koh, C. A., Sum, A. K.,Sloan, E. D. 2012. State of the art: Natural gas hydrates as a natural resource. Journal of Natural Gas Science and Engineering **8**: 132-138.

Mao, W. L., Koh, C. A.,Sloan, E. D. 2007. Clathrate hydrates under pressure. Physics Today **60**(10): 42-47.

Marinhas, S., Delahaye, A., Fournaison, L., Dalmazzone, D., Furst, W.,Petitet, J. P. 2006. Modelling of the available latent heat of a CO2 hydrate slurry in an experimental loop applied to secondary refrigeration. Chemical Engineering and Processing **45**(3): 184-192.

Sloan, E. D. 1998. Clathrate hydrates of natural gases. New York, Marcel Dekker Inc.

Sloan, E. D.,Koh, C. A. 2008. Clathrate hydrates of natural gases. New York, Taylor & Francis CRC Press.

Youssef, Z., Delahaye, A., Huang, L., Trinquet, F., Fournaison, L., Pollerberg, C.,Doetsch, C. 2013. State of the art on phase change material slurries. Energy Conversion and Management **65**(0): 120-132.

Zhang, P.,Ma, Z. W. 2012. An overview of fundamental studies and applications of phase change material slurries to secondary loop refrigeration and air conditioning systems. Renewable and Sustainable Energy Reviews **16**(7): 5021-5058.